Rescue of defective G protein–coupled receptor function in vivo by intermolecular cooperation

Adolfo Rivero-Müller[a], Yen-Yin Chou[b,c], Inhae Ji[d], Svetlana Lajic[b], Aylin C. Hanyaloglu[b], Kim Jonas[b], Nafis Rahman[a], Tae H. Ji[d], and Ilpo Huhtaniemi[a,b,1]

[a]Department of Physiology, University of Turku, 20520 Turku, Finland; [b]Department of Reproductive Biology, Hammersmith Campus, Imperial College London, London W12 0NN, United Kingdom; [c]Institute of Clinical Medicine, National Cheng Kung University Medical College and Hospital, Tainan, 701 Taiwan; and [d]Department of Chemistry, University of Kentucky, Lexington, KY 40506-0055

Edited by Robert J. Lefkowitz, Duke University Medical Center, Durham, NC, and approved October 26, 2009 (received for review June 18, 2009)

G protein–coupled receptors (GPCRs) are ubiquitous mediators of signaling of hormones, neurotransmitters, and sensing. The old dogma is that a one ligand/one receptor complex constitutes the functional unit of GPCR signaling. However, there is mounting evidence that some GPCRs form dimers or oligomers during their biosynthesis, activation, inactivation, and/or internalization. This evidence has been obtained exclusively from cell culture experiments, and proof for the physiological significance of GPCR di/oligomerization in vivo is still missing. Using the mouse luteinizing hormone receptor (LHR) as a model GPCR, we demonstrate that transgenic mice coexpressing binding-deficient and signaling-deficient forms of LHR can reestablish normal LH actions through intermolecular functional complementation of the mutant receptors in the absence of functional wild-type receptors. These results provide compelling in vivo evidence for the physiological relevance of intermolecular cooperation in GPCR signaling.

di/oligomerization | luteinizing hormone receptor | testis | transgenic mice | fertility

G protein–coupled receptors (GPCRs) mediate cellular signaling for a variety of stimuli, including light, ions, odorants, taste, neurotransmitters, and hormones, and they represent one of the largest gene families, with ≈1,000 members (≈3% of the genome). GPCR dysfunction underlies many diseases, and ≈40% of currently used drugs function through GPCRs, emphasizing their importance (1, 2).

GPCRs have a common central core structure with a serpentine seven-transmembrane domain (7TM), and its conformational modulation after ligand binding transmits the activation signal through the cell membrane, mainly by activating heterotrimeric G proteins. In turn, G proteins trigger a cascade(s) of intracellular responses, including generation of second messengers, activation of kinases, and, finally, changes in gene expression. The dogma has been that upon GPCR activation, one ligand molecule binds to one receptor molecule. An alternative concept entails GPCR di/oligomerization with receptor(s) of the same (homodimerization) or a different (heterodimerization) type. Clear evidence for the functional role of GPCR homo- and heterodimerization was first obtained for class C receptors, such as $GABA_B$, taste ($T1R_{1–3}$) metabotropic glutamate (mGluR), and calcium-sensing receptors, where only dimers are involved in signal transduction (3, 4). The information about the functional significance of in vivo di/oligomerization of the large class A GPCRs is controversial. Some class A GPCRs may function as monomers, as suggested by their ability to become activated when forced into the monomeric conformation (5). Conspicuously, the information about the different modes of GPCR interactions has so far been obtained in cell culture experiments, and their significance in the physiological context in vivo remains open.

Besides signal transduction, some GPCRs are detected as di/oligomers during their biosynthesis before membrane delivery (6–8) and ligand binding (9, 10), and during their internalization after signal transduction (11, 12). Likewise, di/oligomerization could explain the negative or positive receptor cooperativity (13, 14), reconstitution of activation by mutant receptors (15, 16), and ligand promiscuity (17). The interactions of some GPCR dimers are covalent (18–22), noncovalent (interactions involving the transmembrane domains or coiled-coil interactions; reviews, e.g., in refs. 2 and 23), or both (24). Noncovalent interactions are likely to form very transient interactions (25), fueling the debate on both the existence and functional significance of dimerization for class A GPCRs (26–29). Possibly, a liganded receptor interacts sequentially with another or multiple nonliganded receptors in its vicinity, pushing the equilibrium from an "active" to an "active–active" state (30, 31). This could explain how the hypothetical cis (Fig. 1*A*) and trans (Fig. 1*B*) conformations of GPCRs result in G protein activation (32, 33). The latter "intermolecular noncovalent cooperation," a term previously coined by Ng et al. (34), has a broad implication in biological systems where a specific signal could be rapidly amplified, with minimal ligand binding, yet maintaining the specificity of action.

There is recent functional evidence that the class A GPCRs for glycoprotein hormones [i.e., of LH/choriongonadotropin (hCG), FSH, and TSH] could transduce their signal in cultured cells as di/oligomers by *trans*-activation (8, 10, 14, 35) (Fig. 1*B*), henceforth termed intermolecular cooperation. In this study, we used LHR, a glycoprotein hormone receptor, as a model to determine whether GPCR activation through intermolecular cooperation is physiologically relevant in vivo.

Results

Experimental Design and Rationale. We hypothesized that coexpression of binding- and signaling-deficient LHR mutants in transgenic (TG) mice in the absence of functional endogenous receptor (i.e., in the *LHR* knockout background) could restore LHR function by functional complementation. We selected two LHR mutant receptors for their inability to bind the ligand (LH or hCG) or to transduce signaling after ligand binding. The first mutant receptor (LHR^{LH-}) harbored an inactivating Cys^{22} to Ala^{22} mutation in the ligand binding extracellular domain (35, 36). The second mutant (LHR^{cAMP-}) contained a deletion of TM helices 6 and 7 in exon 11 (amino acids deleted from Val^{553} to Ala^{689}), and it was chosen because of involvement of the deleted region in G protein coupling and second messenger generation (37). Furthermore, this region is a hotspot for inactivating *LHR* mutations (38).

Author contributions: A.R.-M., S.L., T.H.J., and I.H. designed research; A.R.-M., Y.-Y.C., I.J., S.L., A.C.H., and K.J. performed research; A.R.-M., Y.-Y.C., I.J., A.C.H., N.R., T.H.J., and I.H. analyzed data; and A.R.-M., Y.-Y.C., S.L., A.C.H., T.H.J., and I.H. wrote the paper.

The authors declare no conflict of interest.

This article is a PNAS Direct Submission.

See Commentary on page 1819.

Freely available online through the PNAS open access option.

[1]To whom correspondence should be addressed. E-mail: ilpo.huhtaniemi@imperial.ac.uk.

This article contains supporting information online at www.pnas.org/cgi/content/full/0906695106/DCSupplemental.

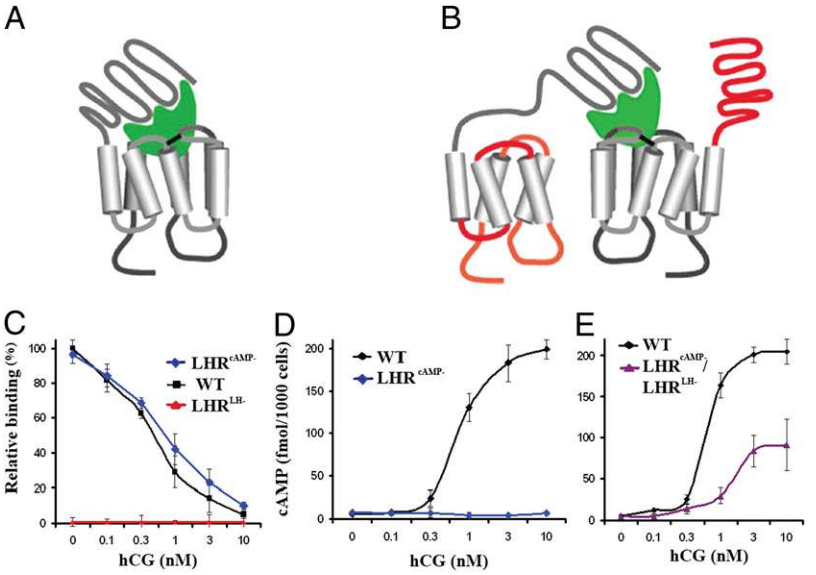

Fig. 1. Demonstration of intermolecular cooperation and di/oligomerization on binding- and signaling-deficient LHR mutants in cultured cells. (*A* and *B*) Schematic presentation of intramolecular (cis) and intermolecular (trans) activation of GPCRs. (*A*) When a hormone (green) binds to its WT receptor, the occupied receptor activates itself to generate a signal(s) (5). (*B*) Alternatively, a GPCR complexed with hormone may activate another GPCR molecule, as evidenced by intermolecular activation of signaling-deficient mutant (LHR^{cAMP-} with red connecting loops) by binding-deficient mutant (LHR^{LH-} with red extracellular domain) when both mutants are coexpressed in a cell (33, 35, 36). (*C–E*) Cell culture experiments on ligand binding and cAMP generation of the LHR mutants. (*C*) Binding-deficient receptor (LHR^{LH-}; red line) was incapable of displaying specific binding of [^{125}I]-hCG in the presence of increasing concentrations of unlabeled hCG (0–10 nM). In contrast, WT (black line) and signaling-deficient LHR (LHR^{cAMP-}; blue line) bound [^{125}I]-hCG specifically and with similar apparent affinity. (*D*) WT LHR (black line) produced cAMP in response to hCG stimulation. However, neither the signaling-deficient (LHR^{cAMP-}, blue line) nor the binding-deficient (LHR^{LH-}, superimposed with the former) mutant produced cAMP. (*E*) When both (LHR^{LH-} and LHR^{cAMP-}) mutants were coexpressed in HEK-293 cells, cAMP production was partially restored in response to hCG (purple line) as compared to WT LHR (black line). One of three experiments with similar results transfecting with BAC-*LHR* clones is shown. Each point is the mean ± SD of triplicate incubations. Experiments with cDNA clones produced similar results.

Intermolecular Cooperation and Di/Oligomerization of the Mutant LHRs in Cell Culture. To confirm that the mutant receptors on their own were inactive and could cooperate intermolecularly, the mutant *LHR* cDNAs, and BAC clones harboring the same *LHR* mutants (*SI Experimental Procedures* and Fig. S1), were tested in transfected HEK-293 cells. As expected, LHR^{LH-} showed no specific ligand binding and LHR^{cAMP-} no signaling, but when the two receptor mutants were coexpressed, the cAMP response to hCG stimulation was partially restored (Fig. 1 *C–E*), confirming earlier reports with similar receptor mutants (35) or even by more defective mutants, such as the exo-domain of the FSHR linked to a cell membrane phospholipid which is capable of activating a binding-deficient mutant (36).

The expected transfer of the mutated receptors to the plasma membrane was studied by confocal immunofluorescence analysis. cDNAs encoding the two mutant receptors were N-terminally tagged with HA or FLAG, respectively, after the signal peptide (referred to as HA-LHR^{LH-} and FLAG-LHR^{cAMP-}). Fig. 2*A* clearly shows that the WT and both mutant receptors, HA-LHR^{LH-} and FLAG-LHR^{cAMP-}, are localized at the cell surface. Hence, the lack of transfer to the cell membrane is not the reason for the total lack of function of the two LHR mutants when expressed on their own (Fig. 1 *C* and *D*).

To demonstrate physical interaction (di/oligomerization) between the receptor mutants, HEK-293 cells expressing either or both of the tagged LHR mutants (see above) were lysed, followed by immunoprecipitation (IP) of the FLAG-tagged receptor (*Methods*). Whereas FLAG-tagged receptors (FLAG-LHR^{cAMP-}) could be observed after all IPs with the FLAG antibody (Fig. 2*B*), HA-tagged LHR^{LH-} could only be detected in immunoprecipitates from cells coexpressing both mutants with bands representing both monomers and SDS-resistant dimers (Fig. 2*C*, lane 5). A control sample containing combined extracts of cells expressing one of the mutants separately, combined after lysis, indicated that the LHR^{LH-}–LHR^{cAMP-} interaction can only occur in cells expressing both mutants, and not as a conglomeration artifact (Fig. 2*C*, lane 4). In another control experiment, we coexpressed FLAG-LHR^{cAMP-} and HA-β2-adrenergic receptor (β2-AR) (Fig. 2 *B* and *C*, lane 6). FLAG antibody immunoprecipitation demonstrated presence of LHR di/oligomers, but no clear evidence for LHR-β2AR association could be shown upon immunoblotting with HA antibody. Hence, LHR di/oligomerization under these conditions was specific and not a random phenomenon with other GPCRs.

To exclude the possibility that the apparent lack of activation of the mutant receptors as monomers depends on a low level of expression, we transfected HEK-293 cells with increasing amounts (up to 100 ng) of cDNAs encoding LHR^{cAMP-} and LHR^{LH-} (*SI Results* and Fig. S2). No cAMP generation was found either basally or in the presence of maximally stimulating hCG level (5 nM), indicating that the mutant receptors, even when highly expressed, are not able to restore signaling as monomers. The possibility of their activation as heterodimers with another functional GPCR was studied by cotransfecting the LHR^{cAMP-} mutant with the β2-AR to HEK-293 cells (*SI Results* and Fig. S2). No activation of cAMP signaling was found either basally or in response to hCG. This finding corroborates the lack of LHR activation in the TG mice expressing one of the mutant LHRs (see below).

Generation of TG Mice. To investigate the possibility of LHR activation through intermolecular cooperation in vivo, we set out to modify bacterial artificial chromosome (BAC) clones containing the entire mouse *LHR* by homologous recombination, to obtain two mutant clones containing the same mutations as described above (Fig. S1). The use of BAC clones ensures normal spatiotemporal expression of the TG *LHR* mutants. Each BAC also contained a reporter gene for bicistronic expression, *Dicosoma* sp. red fluorescent protein (RFP) or enhanced cyan fluorescent protein (eCFP), respectively, downstream of the LHR^{cAMP-} and LHR^{LH-} genes, to be used for expression profiling and genotyping (for details, see *SI Experimental Procedures* and Fig. S1).

Both *LHR* mutant BACs were then microinjected into fertilized FVB/N mouse oocytes by standard procedures. As the definitive experiments needed to be carried out in the *LHR-null* (LuRKO) background, we designed a breeding strategy to create intercrosses of each of the TG *LHR* mutants alone or together in the homozygous LuRKO background ($LHR^{LH-/cAMP-}$) (39). The mutant LHR BAC clones contained modified areas differing from the WT or LuRKO loci, which could be used for genotyping of the TG animals, as well as to make sure that the transgenes did not integrate to the WT or LuRKO genomic alleles by recombination (Fig. S1). The transgene copy numbers were similar in the LHR^{LH-} (3–11) and LHR^{cAMP-} (2–8) lines (Table S1).

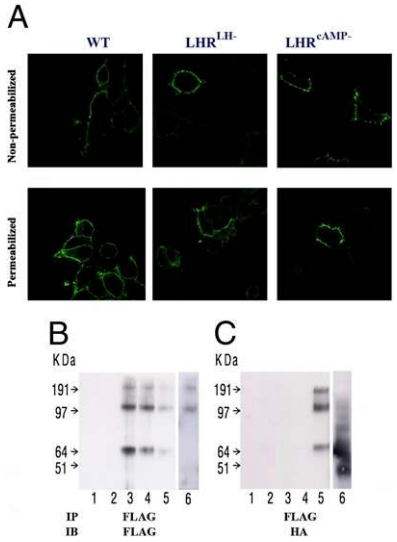

Fig. 2. LHR cellular localization and di/oligomerization. (*A*) Cell surface expression. HEK-293 cells expressing tagged-LHRs (HA-WT, HA-LHR^{LH-}, or FLAG-LHR^{cAMP-}) were immunostained using anti-HA or anti-FLAG antibodies, respectively, and secondary antibodies labeled with fluorescent dyes, and analyzed by confocal microscopy. All three receptors (WT and mutants) could be detected on the cell surface as shown on nonpermeabilized cells (*Upper*), while some receptor immunoreactivity was detected in the ER of permeabilized cells (*Lower*). This proves that the WT and mutant receptors are transported to the cell surface. (*B* and *C*) Dimerization/oligomerization of mutant mLHRs. HEK-293 cells were transiently transfected with FLAG-tagged signaling-deficient (FLAG-LHR^{cAMP-}) and HA-tagged binding-deficient (HA-LHR^{LH-}) mutant constructs. Lysates were prepared and subjected to immunoprecipitation (IP) with anti-FLAG antibody. Thereafter, the immunoprecipitates were resolved by SDS/PAGE under reducing conditions, and immunoblots (IB) were probed with either anti-FLAG antibody (*B*) or anti-HA antibody (*C*). Both monomeric and higher molecular weight LHR complexes were detected. These data indicate that FLAG-LHR^{cAMP-} mutant interacts with HA-LHR^{LH-} mutant. The lanes are: 1, control vector (pcDNA); 2, HA-LHR^{LH-}; 3, FLAG-LHR^{-cAMP}; 4, combined lysates from separately FLAG-LHR^{-cAMP} and HA-LHR^{-LH} transfected cells; 5, coexpressed FLAG-LHR^{-cAMP} + HA-LHR^{-LH}; 6, coexpressed FLAG-LHR^{cAMP-} + HA-β2-AR (different experiment with identical conditions).

LHR Mutant Expression in Vivo and Phenotypes of the TG Animals. The expression of both mutant *LHR* BAC transgenes at mRNA level was mainly confined to the gonads, with a low level of expression in the brain (Fig. 3*A*), where *LHR* expression has been previously reported (40). To determine the transgene expression at protein level, we analyzed the expression of the reporter genes [*Discosoma* sp. red fluorescent protein (RFP) or enhanced cyan fluorescent protein (eCFP)] (Fig. 4). Due to the presence of high levels of cholesterol and its derivates, there was high autofluorescence background in the gonads, particularly in testicular Leydig cells (LC), which made it difficult to detect the reporter fluorescent proteins. To differentiate the reporter fluorescence from background, and to increase the signal, immunofluorescence of fixed testis sections was performed by using specific antibodies against RFP or GFP (which also detects eCFP). This confirmed that the expression of both transgenes was confined only to LC in the testes (Fig. 4). In brain, the low expression observed at mRNA level (Fig. 3*A*) was undetectable at protein level by immunohistochemistry.

The testes of LHR^{LH-} and LHR^{cAMP-} mutant mice were analyzed for their ability to specifically bind [^{125}I]-hCG. Testis homogenates of LHR^{cAMP-} and LHR$^{LH-/cAMP-}$ mice showed similar levels of binding as those of WT mice, whereas the LHR^{LH-} testes showed no hCG binding, as expected (Figs. 3 *B* and *C*). While LHR mRNA levels in the single TG testes were half of that of the WT testes, they were over 2-fold higher in the double-TG testes (Table S2).

Both receptor mutants (LHR^{cAMP-} and LHR^{LH-}) in the LuRKO background presented with phenotypes indistinguishable from LuRKO animals (39, 41), with arrested postnatal sexual maturation, cryptorchid testes, small and poorly developed accessory sex organs, LC hypoplasia, spermatogenic arrest at the round spermatid stage (Figs. 4 and 5 *A–C*) and very low serum testosterone levels (Fig. 5*F*). These results confirm that the mutant LHRs are completely inactive on their own also in vivo, and demonstrate that the mutant TG clones do not interact with the LuRKO alleles.

In striking contrast to the single mutants in LuRKO background, males expressing both *LHR* mutants (LHR$^{LH-/cAMP-}$) in this background showed complete rescue of the WT phenotype. The testes of these mice were descended to the scrotum and had normal weight and size. Accessory sex organs also were fully developed with normal size (Fig. 4 *D* and *E*, *SI Results*, and Table S3); serum testosterone levels were in the WT range (Fig. 5*F*). LC volume density and seminiferous tubule diameters were also similar in LHR$^{LH-/cAMP-}$ and WT mice (*SI Results* and Table S4).

Further evidence for functionality of LHR signaling in the LHR$^{LH-/cAMP-}$ mice was provided by the serum LH levels, which, albeit slightly higher than in WT mice, were only approximately one-quarter of those measured in LuRKO mice, as the sign of gonadal negative feedback effect on gonadotropin secretion (Fig. 5*F*). Full spermatogenesis and normal-sized interstitial LC islets were observed by histological analysis of the testes (Fig. 5 *D* and *E*). Furthermore, the LHR$^{LH-/cAMP-}$ males were fertile and sired similar numbers of pups as WT males [7.1 ±1.9 vs. 7.5 ± 1.3, respectively (mean ± SD; n = 3–4)].

Finally, as clear evidence that the rescue of the phenotype was due to LHR-signaling in LCs, we measured the expression of two LH-dependent, LC-specific genes [steroidogenic acute regulatory protein (*StAR*; GenBank no. NM_011485) and P450, family 17, subfamily a, polypeptide 1 (*Cyp17a1*; GenBank no. NM_007809)] (42), by quantitative RT-PCR (qPCR), where both genes were highly expressed in WT and LHR$^{LH-/cAMP-}$, but at very low level in LHR^{LH-}, LHR^{cAMP-}, or LHR$^{-/-}$ mice (*SI Results* and Table S5). There was no evidence for residual activity of either of the mutant receptors alone even when these mice had 10-fold higher serum LH levels than control WT animals throughout their life, without significant testosterone production or LH-dependent gene response.

Discussion

Our findings demonstrate cooperation between GPCRs because this is the only possibility for a binding- and a signaling-deficient receptor to restore normal hormone action in the physiological context. The evidence for di/oligomerization upon GPCR activation is still exclusively based on data from cell cultures and immunoblots of tissue extracts, which has left the functional significance of this phenomenon open and controversial. In earlier studies on cultured living cells, coexpression of binding- and signaling-deficient LHR mutants was able to partly rescue the intracellular cAMP response (33, 35), as was also confirmed here (Fig. 1). Although cAMP is the key second messenger in LHR signaling, and a universal product of the activation of all GPCRs, these experiments cannot resolve how well the functional complementation can restore all physiologically important aspects of LHR function in vivo. Our current findings provide strong evidence that intermolecular cooperation is sufficient to restore all physiologically essential functions of LHR. To what extent this finding can be generalized to other GPCRs remains to be studied.

LHR expression from BACs was directed in a tissue-specific manner mainly to gonads, and more specifically to LC in male mice. Because neither receptor mutant alone was capable of restoring the WT phenotype, the result proves that both of them are functionally inactive also in vivo despite high LH levels (Fig. 5*F*). Moreover, the LHR^{cAMP-} mutant was able to bind hCG in testis homogenates without any phenotypic signs of LHR activa-

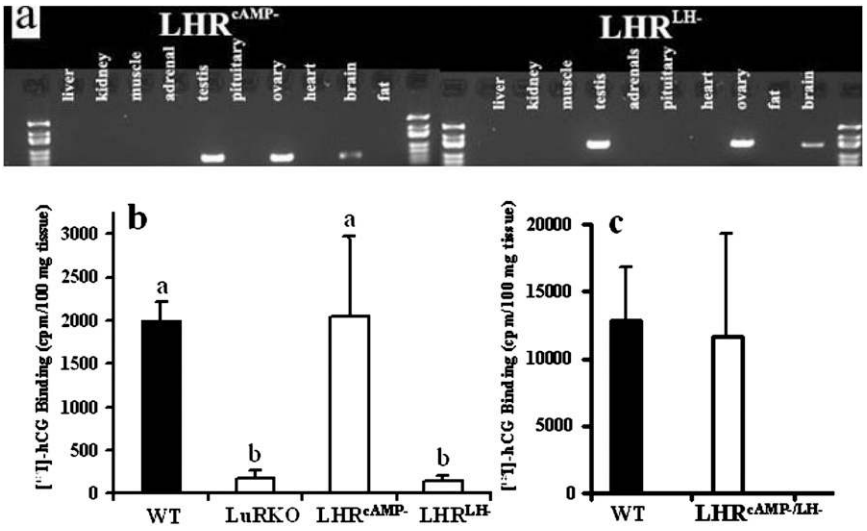

Fig. 3. Expression of the LHR^{cAMP-} and LHR^{LH-} BAC transgenes in male mice. (*A*) Expression of mRNA of the transgenes (LHR^{cAMP-} and LHR^{LH-}) in different tissues of TG mice as analyzed by RT-PCR, showing strong specific expression in gonads (product sizes 559 and 960 bp, respectively) and weak expression in brain. (*B*) Specific [^{125}I]-hCG binding to testis homogenates of WT, LuRKO, LHR^{cAMP-}, and LHR^{LH-} mice (n = three per group), as well as, in a separate binding assay, WT (n = 4) and $LHR^{LH-/cAMP-}$ (n = 2) mice (*C*). Each bar is the mean + SD. Different letters above the bars in *B* indicate that these levels differ significantly (P at least <0.05).

tion, and the LHR^{LH-} mutant was not able to bind hCG. Previous cell culture studies on expression of complementary receptor mutants have shown that the observed intermolecular cooperation was not due to rescue of one mutant, trapped in the endoplasmic reticulum (ER), by the other to the cell membrane, but to direct interaction of two complementary mutants at the cell membrane (33, 35), as was also the case with the intermolecular cooperation of FSHRs (36). Furthermore, overexpression of the mutant receptors alone in HEK-293 cells could not demonstrate any cAMP signaling activity, indicating that the mutant receptors do not attain spurious activation as monomers even when overexpressed.

Further evidence that the intermolecular cooperation of LHRs is not the result of trafficking rescue through the ER by another receptor, but of direct cooperation between these mutants, is presented by the surface expression of both mutants separately. Moreover, immunoprecipitation of one tagged LHR associated with the complementary receptor indicated that these receptors physically interact with each other at the molecular level, and form homo-di/oligomers (~120 KDa, ~240 KDa, and higher magnitude), similar to a recent report where LHR di/oligomers were detected by BRET (8).

When both receptor mutants were coexpressed in TG mice in the LuRKO background, LHR signaling was restored to such an extent that it was able to normalize LC differentiation, gonadal development, sexual maturation, androgen production, and spermatogenesis. Finally, the mice were fertile and sired similar numbers of pups with WT controls. Interactions between the LHR mutants and other GPCRs are unlikely because the mice carrying single *LHR* mutations did not present any recovery of phenotype, and signaling-deficient LHR mutant overexpressed in HEK-293 cells with another GPCR (i.e., the β2-AR) did not dimerize or generate cAMP response. It is therefore likely that the homo-di/oligomer cooperation detected represents a normal physiological phenomenon in the activation and intracellular signaling of the LHR, and might also apply to other structurally similar GPCRs such as FSHR and TSHR. However, our findings do not exclude the possibility of functional receptor monomers; for example, the single α/β-hCG-LHR fusion protein forms a constitutively active complex (43). Such a configurational flexibility is surprising because receptors maintain high ligand specificity while being able to form complexes with their ligands in different arrangements, e.g., gonadotropin α-

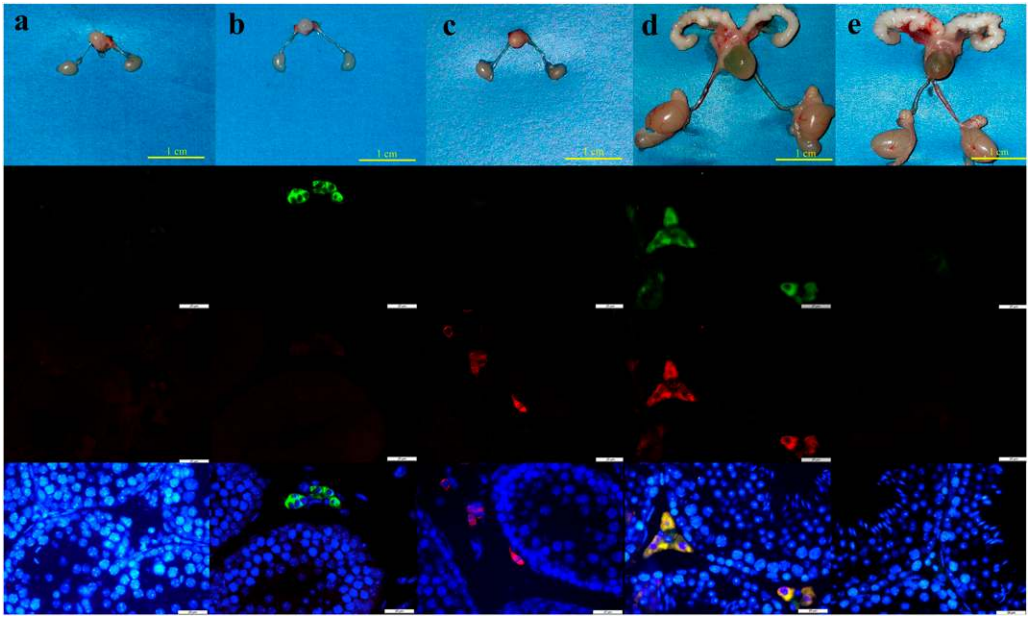

Fig. 4. Gonadal and genital phenotypes: macroscopic and microscopic appearance of the WT and mutant male mice. (*Top*) Testes and accessory sex organs (from left to right) of LuRKO mice (*A*) and mice expressing in the LuRKO background LHR^{LH-} (*B*), LHR^{cAMP-} (*C*), both transgenes ($LHR^{LH-/cAMP-}$) (*D*), and WT mice (*E*). (*Middle*) Immunofluorescence of the reporter genes (eCFP, green, corresponding to LHR^{LH-}; RFP, red, corresponding to LHR^{cAMP-}) specifically expressed in Leydig cells (LC). (*Bottom*) Merged pictures of the two reporter genes, showing coexpression of the two transgenes in LC of $LHR^{LH-/cAMP-}$ mice. (Scale bars: *Top*, 1 cm; *Middle* and *Bottom*, 25 μm).

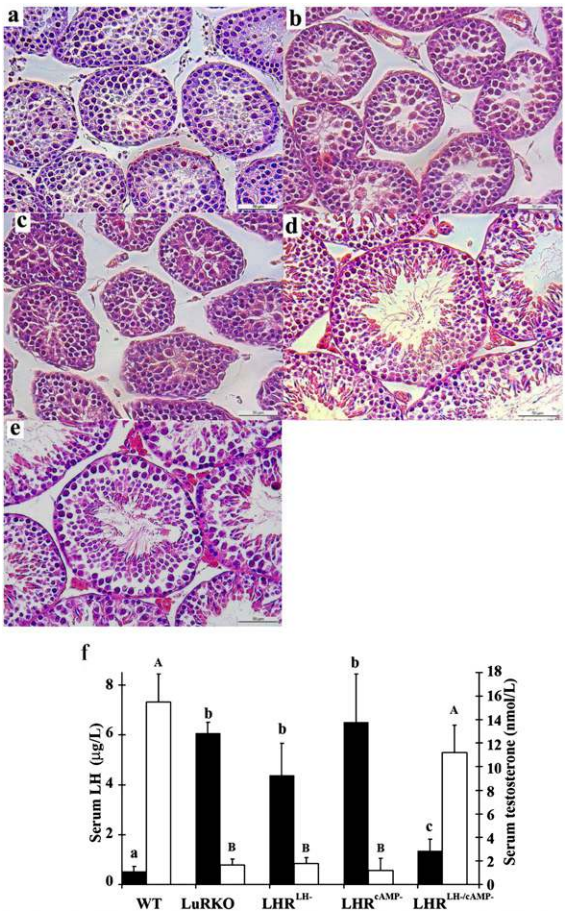

Fig. 5. Testicular histology and serum hormone levels of the WT and mutant mice. (*A*) LuRKO mice. (*B–D*) Mice expressing in the LuRKO background LHR^{LH-}, LHR^{cAMP-}, or both transgenes ($LHR^{LH-/cAMP-}$), respectively. (*E*) WT mice. LuRKO mice and the inactivating mutants alone display the same histology with Leydig cell hypoplasia, narrow seminiferous tubules, and spermatogenesis arrested at the round spermatid stage. When both deficient receptors were coexpressed in the LuRKO background, testicular histology was indistinguishable from WT males. (Scale bar: 50 μm.) (*F*) Serum LH (filled bars) and testosterone (open bars) in, from left to right, WT, LuRKO, LHR^{LH-}, LHR^{cAMP-}, and $LHR^{LH-/cAMP-}$ mice. Each bar denotes the mean ± SD of measurements from at least four mice. Different letters above the bars indicate that these levels differ significantly (P at least <0.05).

and β-chains tethered into various dimeric or tetrameric orientations retain the bioactivity of the hormone–receptor complexes (44, 45). To what degree such conformations recapitulate the fully physiological response remains to be studied. What is becoming clear is that LHR and FSHR di/oligomers are already formed in the ER during their biosynthesis (8, 10).

Our approach to studying the GPCR intermolecular cooperation in vivo was made possible by the availability of the LuRKO mouse (39). It was crucial that the mutant LHRs were expressed in the absence of functional WT receptors and completely inactive on their own. It was also important to have a model where the phenotype is so specific and clear that only the expected intermolecular cooperation of mutant receptors could rescue it.

Earlier cell culture studies have revealed quantitative difference in the cAMP and phosphoinositide responses of gonadotropin receptors upon their *cis*- and *trans*-activation (33, 36, 46), but more pronounced qualitative differences in the responses to the two modes of receptor activation are possible. The only difference we found between the WT and $LHR^{LH-/cAMP-}$ mice was the 2-fold elevation of LH in the latter, suggesting that the *trans*-activated receptor complex is slightly less sensitive or less responsive to stimulation than the WT receptor. Lower binding affinity, smaller receptor density, or less efficient signaling are possible explanations for the difference. This was expected from the rescuing results on cultured cells where only partial cAMP activation is achieved.

The intermolecular cooperation upon LHR activation might provide answers to some questions hotly debated about GPCR di- and oligomerization (26–29), because it suggests that the receptors, when in close physical contact, can activate another or several others in their vicinity after ligand binding. It could also contribute to the "spare receptor" concept, i.e., that a small proportion of liganded receptors is sufficient to evoke full biological response (47). Most importantly, however, intermolecular cooperation may also occur between other GPCRs, adding to the complexity of these receptors interactions and their diversity in biological systems.

Methods

LHR Mutants. The mouse *LHR* cDNA was kindly provided by Lutz Birnbaumer (National Institutes of Health/National Institute of Environmental Health Sciences). *LHR* mutants were created by oligonucleotide-mediated site-directed mutagenesis using the QuikChange II Site-Directed Mutagenesis Kit (Stratagene) according to the manufacturer's instructions, and cloned into the expression vector pDNA3.1(–) (Invitrogen) (see *SI Experimental Procedures* for details and oligonucleotide sequences).

The bovine prolactin signal peptide was inserted by Red/ET recombination as for the BAC clone carrying the same mutant (see below). The entire coding region of each construct was sequenced to verify fidelity of the constructs.

BACs and Recombination. A BAC clone carrying the entire mouse *LHR* gene (RPCI23-18D7) was obtained from BAC PAC resources of Oakland Children's Hospital in *E. coli* strain HS996. BAC point and deletion mutants were constructed by Red/ET recombination (GeneBridges). IRES-DsRed and IRES-eCFP (modified from the original Clontech vectors) were cloned into the mutated *LHR* BACs by Red/ET recombination (48) (see *SI Experimental Procedures* for primer sequences). BAC DNA was propagated in bacteria by standard procedures, purified, linearized, gel-purified and injected into the pronucleus of fertilized mouse oocytes using standard procedures. See *SI Experimental Procedures* for additional details about experimental settings and oligos.

Cell Cultures. Human embryonic kidney (HEK) 293 cells were maintained in T75 flasks at 5% CO_2 in a culture medium consisting of Dulbecco's Modified Eagle's Medium (Sigma) and 10% FBS. Transfections were carried out with Lipofectamine 2000 (Invitrogen). Analyses of activity and immunoprecipitations were performed 48 h after transfections.

LHR binding measurements were carried out with [125I]-hCG as label; further details are presented in *SI Experimental Procedures*.

Immunofluorescence Staining of Tagged Receptors by Confocal Imaging. Visualization of the tagged LHR molecules was carried out using indirect immunofluorescence microscopy of HEK-293 cells stably transfected with *N*-terminally tagged LHR HA-WT, HA-LHR^{LH-}, or FLAG-LHR^{cAMP-}. Surface receptors were labeled with a rabbit anti-FLAG antibody or mouse anti-HA antibody using standard methods (see details in *SI Experimental Procedures*).

Immunoprecipitation. HEK-293 cells expressing either or both *LHR* mutants were collected using lysis buffer with protease inhibitors (50 mM Tris-HCl, pH 7.4, with 150 mM NaCl, 1 mM EDTA, and 1% TRITON X-100). The extracts were incubated on ice for 20 min followed by centrifugation for 15 min at maximal speed. For coimmunoprecipitation of differentially tagged LHRs, cell lysates were incubated overnight with anti-FLAG agarose affinity gel (A2220; Sigma) and then eluted with FLAG peptide (F4799; Sigma). Immunoprecipitates were separated by SDS-polyacrylamide-gel electrophoresis (SDS/PAGE) under reducing conditions, electroblotted onto a nitrocellulose membrane, probed with either an anti-FLAG antibody (F7425; Sigma) or an anti-HA antibody (sc-805; Santa Cruz), and horseradish peroxidase-conjugated goat anti-rabbit IgG (DAKO). The immunoreactive bands were visualized using an ECL detection system (Amersham Biosciences).

Mice. Founder mice were used for generation of heterozygous lines with phenotypes indistinguishable from WT littermates. Both TG lines were then intercrossed with heterozygous *LHR* knockout mice (LuRKO) (39), to create $LHR^{LH-}/LHR^{-/-}$, $LHR^{cAMP-}/LHR^{-/-}$, and $LHR^{LH-/cAMP-}/LHR^{-/-}$ mice. The mice were kept in specific pathogen-free conditions, 2–4 per cage, in controlled

conditions of light (12 h light, 12 h dark) and temperature (21 ± 1 °C) in the animal facility of the University of Turku. The mice were fed with mouse chow Special Diet Service RM-3 (E, soy free; Whitham) and tap water ad libitum. The University of Turku Ethical Committee on Use and Care of Animals approved all procedures of the current experiments. In all experiments WT and heterozygous littermates were used as controls. The animals were killed by overdose of Avertin and cardiac puncture was used for blood collection. Tissues were dissected out, weighed, and snap-frozen in liquid nitrogen, or fixed in 4% paraformaldehyde.

Immunofluorescence of Histological Sections. Whole-mount fixed testis sections were boiled in citric buffer (10 mM sodium citrate, 0.05% Tween-20, pH 6.0) for 10 min, washed and blocked with 10% normal goat serum (NGS) in PBS. Double immunofluorescent staining was performed using standard protocols and commercial mouse anti-RFP and rabbit anti-GFP (which also detects eCFP) antibodies (both MBL International). As secondary antibodies (Molecular Probes), goat anti-rabbit conjugated to Alexa Fluor-488 (green) for eCFP and goat anti-mouse Alexafluor-594 (red) for RFP were used. Nuclei were permeabilized in the last wash with PBS-Triton (0.1%) and stained with DAPI (Vector Laboratories) before mounting with VECTASHIELD antifading medium (Vector Laboratories) (see *SI Experimental Procedures* for additional details about experimental settings). Images were captured on a Leica DMRBE fluorescent microscope (Leica Microsystems), imaged with a CCD camera using IM500 (Leica) and cropped in Adobe Photoshop.

RT-PCR and Genotyping. Standard protocols were followed. Briefly, RT-PCR amplification of total mRNA extracted from different tissues and purified by RNeasy kit (Qiagen) was performed with AMV-reverse transcriptase (Promega) following the manufacturer's instructions, using primer pairs F1 and R1 (*SI Experimental Procedures*). PCR was performed using BioTools polymerase and buffer. The presence of the transgenes was determined by screening tail DNA using the PCR primer pairs shown in *SI Experimental Procedures*.

Quantitative RT-PCR (qPCR). Isolated mRNA from tissue or cell culture samples where analyzed by standard protocols using a SYBR-green kit (DyNAmo; Finnzymes) and a Chomo4 thermo-cycler (Bio-Rad). Primer details are in the *SI Experimental Procedures*.

Statistical Analyses. ANOVA was used for statistical analyses, followed by Tuckey–Kremer multiple comparisons post hoc test to identify the groups differing. All numerical data are presented as the mean ± SD, and $P < 0.05$ was considered statistically significant.

ACKNOWLEDGMENTS. We thank Dr. Petteri Ahtiainen for his help with RT-PCR and fruitful conversations, Dr. Veronika Mamaeva for all the help and useful comments, and Dr. Sonia Bourguiba for sharing her expertise in immunofluorescence and real-time PCR. Nina Messner and Heli Niittymäki are thanked for their technical assistance in microinjection and animal husbandry work. This study was supported by a Centre of Excellence Grant from The Academy of Finland, a Program Grant from The Wellcome Trust, and in part from National Institute of Health grants.

1. Drews J (2000) Drug discovery: a historical perspective. *Science* 287:1960–1964.
2. Bulenger S, Marullo S, Bouvier M (2005) Emerging role of homo- and heterodimerization in G-protein-coupled receptor biosynthesis and maturation. *Trends Pharmacol Sci* 26:131–137.
3. Pin JP, et al. (2004) The activation mechanism of class-C G-protein coupled receptors. *Biol Cell* 96:335–342.
4. Kaupmann K, et al. (1998) GABA(B)-receptor subtypes assemble into functional heteromeric complexes. *Nature* 396:683–687.
5. Whorton MR, et al. (2007) A monomeric G protein-coupled receptor isolated in a high-density lipoprotein particle efficiently activates its G protein. *Proc Natl Acad Sci USA* 104:7682–7687.
6. Margeta-Mitrovic M, Jan YN, Jan LY (2000) A trafficking checkpoint controls GABA(B) receptor heterodimerization. *Neuron* 27:97–106.
7. Salahpour A, et al. (2004) Homodimerization of the beta2-adrenergic receptor as a prerequisite for cell surface targeting. *J Biol Chem* 279:33390–33397.
8. Guan R, et al. (2009) Bioluminescence resonance energy transfer studies reveal constitutive dimerization of the human lutropin receptor and a lack of correlation between receptor activation and the propensity for dimerization. *J Biol Chem* 284:7483–7494.
9. Pin JP, Galvez T, Prézeau L (2003) Evolution, structure, and activation mechanism of family 3/C G-protein-coupled receptors. *Pharmacol Ther* 98:325–354.
10. Thomas RM, et al. (2007) Follice-stimulating hormone receptor forms oligomers and shows evidence of carboxyl-terminal proteolytic processing. *Endocrinology* 148: 1987–1995.
11. Jordan BA, Trapaidze N, Gomes I, Nivarthi R, Devi LA (2001) Oligomerization of opioid receptors with beta 2-adrenergic receptors: a role in trafficking and mitogen-activated protein kinase activation. *Proc Natl Acad Sci USA* 98:343–348.
12. Terrillon S, Bouvier M (2004) Roles of G-protein-coupled receptor dimerization. *EMBO Rep* 5:30–34.
13. El-Asmar L, et al. (2005) Evidence for negative binding cooperativity within CCR5-CCR2b heterodimers. *Mol Pharmacol* 67:460–469.
14. Urizar E, et al. (2005) Glycoprotein hormone receptors: link between receptor homodimerization and negative cooperativity. *EMBO J* 24:1954–1964.
15. Lee C, Ji IJ, Ji TH (2002) Use of defined-function mutants to access receptor-receptor interactions. *Methods* 27:318–323.
16. Monnot C, et al. (1996) Polar residues in the transmembrane domains of the type 1 angiotensin II receptor are required for binding and coupling. Reconstitution of the binding site by co-expression of two deficient mutants. *J Biol Chem* 271:1507–1513.
17. Costagliola S, Urizar E, Mendive F, Vassart G (2005) Specificity and promiscuity of gonadotropin receptors. *Reproduction* 130:275–281.
18. Ray K, Hauschild BC (2000) Cys-140 is critical for metabotropic glutamate receptor-1 dimerization. *J Biol Chem* 275:34245–34251.
19. Bazarsuren A, et al. (2002) In vitro folding, functional characterization, and disulfide pattern of the extracellular domain of human GLP-1 receptor. *Biophys Chem* 96:305–318.
20. Giguère V, Gallant MA, de Brum-Fernandes AJ, Parent JL (2004) Role of extracellular cysteine residues in dimerization/oligomerization of the human prostacyclin receptor. *Eur J Pharmacol* 494:11–22.
21. Kunishima N, et al. (2000) Structural basis of glutamate recognition by a dimeric metabotropic glutamate receptor. *Nature* 407:971–977.
22. Romano C, Yang WL, O'Malley KL (1996) Metabotropic glutamate receptor 5 is a disulfide-linked dimer. *J Biol Chem* 271:28612–28616.
23. Kroeger KM, Pfleger KD, Eidne KA (2003) G-protein coupled receptor oligomerization in neuroendocrine pathways. *Front Neuroendocrinol* 24:254–278.
24. Romano C, et al. (2001) Covalent and noncovalent interactions mediate metabotropic glutamate receptor mGlu5 dimerization. *Mol Pharmacol* 59:46–53.
25. Fonseca JM, Lambert NA (2009) Instability of a class a G protein-coupled receptor oligomer interface. *Mol Pharmacol* 75:1296–1299.
26. James JR, Oliveira MI, Carmo AM, Iaboni A, Davis SJ (2006) A rigorous experimental framework for detecting protein oligomerization using bioluminescence resonance energy transfer. *Nat Methods* 3:1001–1006.
27. Bouvier M, Heveker N, Jockers R, Marullo S, Milligan G (2007) BRET analysis of GPCR oligomerization: newer does not mean better. *Nat Methods* 4:3–4, author reply 4.
28. Salahpour A, Masri B (2007) Experimental challenge to a 'rigorous' BRET analysis of GPCR oligomerization. *Nat Methods* 4:599–600, author reply 601.
29. Gurevich VV, Gurevich EV (2008) GPCR monomers and oligomers: it takes all kinds. *Trends Neurosci* 31:74–81.
30. Parnot C, Kobilka B (2004) Toward understanding GPCR dimers. *Nat Struct Mol Biol* 11: 691–692.
31. Kniazeff J, et al. (2004) Closed state of both binding domains of homodimeric mGlu receptors is required for full activity. *Nat Struct Mol Biol* 11:706–713.
32. Jeoung M, Lee C, Ji I, Ji TH (2007) Trans-activation, cis-activation and signal selection of gonadotropin receptors. *Mol Cell Endocrinol* 260-262:137–143.
33. Ji I, Lee C, Song Y, Conn PM, Ji TH (2002) Cis- and trans-activation of hormone receptors: the LH receptor. *Mol Endocrinol* 16:1299–1308.
34. Ng GY, et al. (1996) Dopamine D2 receptor dimers and receptor-blocking peptides. *Biochem Biophys Res Commun* 227:200–204.
35. Lee C, et al. (2002) Two defective heterozygous luteinizing hormone receptors can rescue hormone action. *J Biol Chem* 277:15795–15800.
36. Ji I, et al. (2004) Trans-activation of mutant follicle-stimulating hormone receptors selectively generates only one of two hormone signals. *Mol Endocrinol* 18:968–978.
37. Sangkuhl K, Schulz A, Schultz G, Schöneberg T (2002) Structural requirements for mutational lutropin/choriogonadotropin receptor activation. *J Biol Chem* 277: 47748–47755.
38. Huhtaniemi IT, Themmen APN (2000) Mutations of gonadotropins and gonadotropin receptors: elucidating the physiology and pathophysiology of pituitary-gonadal function. *Endocr Rev* 21:551–583.
39. Zhang FP, Poutanen M, Wilbertz J, Huhtaniemi I (2001) Normal prenatal but arrested postnatal sexual development of luteinizing hormone receptor knockout (LuRKO) mice. *Mol Endocrinol* 15:172–183.
40. Lei ZM, Rao CV, Kornyei JL, Licht P, Hiatt ES (1993) Novel expression of human chorionic gonadotropin/luteinizing hormone receptor gene in brain. *Endocrinology* 132:2262–2270.
41. Ahtiainen P, et al. (2007) Phenotypic characterisation of mice with exaggerated and missing LH/hCG action. *Mol Cell Endocrinol* 260-262:255–263.
42. Huhtaniemi I, et al. (2006) Genetically modified mouse models in studies of luteinising hormone action. *Mol Cell Endocrinol* 252:126–135.
43. Wu C, Narayan P, Puett D (1996) Protein engineering of a novel constitutively active hormone-receptor complex. *J Biol Chem* 271:31638–31642.
44. Kanda M, et al. (1999) Genetic fusion of an alpha-subunit gene to the follicle-stimulating hormone and chorionic gonadotropin-beta subunit genes: production of a bifunctional protein. *Mol Endocrinol* 13:1873–1881.
45. Xing Y, et al. (2001) Alternatively folded choriogonadotropin analogs. Implications for hormone folding and biological activity. *J Biol Chem* 276:46953–46960.
46. Lee C, Ji I, Ji TH (2004) Distinct mechanisms of cAMP induction by constitutively activating LH receptor and wild-type LH receptor activated by hCG. *Endocrine* 25:111–115.
47. Catt KJ, Dufau ML (1973) Spare gonadotrophin receptors in rat testis. *Nat New Biol* 244:219–221.
48. Zhang Y, Buchholz F, Muyrers JP, Stewart AF (1998) A new logic for DNA engineering using recombination in Escherichia coli. *Nat Genet* 20:123–128.

Supporting Information

Rivero-Müller et al. 10.1073/pnas.0906695106

SI Experimental Procedures

LHR cDNA Mutants. Oligonucleotide-mediated site-directed mutagenesis was performed by using the QuikChangeII Site-Directed Mutagenesis Kit (Stratagene) according to the manufacturer's instructions. Clones selected by ampicillin were directly sequenced to verify that they contained the correct mutation. The entire sequence of each mutant cDNA was determined.

The LHR mutants (LHR^{LH-} and LHR^{cAMP-}) as cDNAs were then subcloned into an expression vector pDNA3.1(-) (Invitrogen) between the restriction site of EcoRI and BamHI and tagged with HA or FLAG into the N-terminal coding sequence just after the signal peptide (referred to as FLAG-LHR^{cAMP-} and HA-LHR^{LH-}). The entire coding region of each cDNA construct was sequenced to verify the different modifications.

BACs and Recombination. A BAC clone carrying the entire mouse LHR gene (RPCI23-18D7) was obtained from the BAC PAC resources of Oakland Children's Hospital in *E.coli* strain HS996. The C22A mutation (LHR^{LH-}) was adjusted by a mouse codon usage program (www.entelechon.com). The point mutation in LHR^{LH-} and ΔTM67 deletion in LHR^{cAMP-} were achieved by inserting and replacing a selection/counter selection cassette (*RpsL*-Neo) with single strand oligonucleotides (1) (see below for primer sequences). Bicistronic reporter cassettes were inserted by Red/ET recombination and screened with specific primers. Prolactin signal sequence was inserted by the ALFIRE procedure (2), first by inserting an *RpsL*-Neo cassette flanked by ISce-I restriction sites and homology arms to the bovine PRL signal sequence from a previously described vector (3). All areas of modification were sequenced to ensure correctness. PCR amplification for recombineering was performed using TripleMaster polymerase mix and buffers (Eppendorf). BAC DNA was propagated in bacteria by standard procedures and purified using a Large construct Maxiprep kit (Qiagen), linearized, PFGE gel-purified and injected into the pronucleus of fertilized mouse oocytes using standard procedures. Additional details about the experimental settings and oligos are below.

Tissues for Immunofluorescence, RT-PCR, and Receptor Binding Assays. Blood, testes, seminal vesicles, and other organs were collected, and their weights were recorded. Serum was separated by centrifugation, frozen, and stored at -20 °C until used for hormone assays. After removal, one of each pair of testes was immediately frozen in liquid nitrogen and stored at -70 °C until used for LHR binding and mRNA measurements. The other testis was fixed in freshly prepared 4% paraformaldehyde at 4 °C, dehydrated with ethanol, and embedded in paraffin for immunofluorescence or immunohistochemistry.

Immunofluorescence of Histological Sections. Whole-mount fixed testis sections were boiled in citric buffer (10 mM sodium citrate, 0.05% Tween-20, pH 6.0) for 10 min, washed and blocked with 10% normal goat serum (NGS) in PBS. Then, double immunofluorescent staining was performed using standard protocols and commercial mouse anti-RFP and rabbit anti-GFP (which also detects eCFP) antibodies (both MBL International Antibodies) diluted in PBS (0.05% goat serum) 1:100. Sections were incubated with primary antibodies overnight at 4 °C, and thereafter washed twice in PBS before exposure to the secondary antibodies (1:500) (Molecular Probes), goat anti-rabbit conjugated to Alexafluor-488 (green) for eCFP and goat anti-mouse Alexafluor-594 (red) for RFP, for 1h at room temperature. Nuclei were permeabilized in the last wash with PBS-Triton (0.1%) and stained with DAPI (Vector Laboratories) (dilution 1:10,000) for 5 min before mounting with Vectashield antifading medium (Vector Laboratories). Images were captured on a Leica DMRBE fluorescent microscope (Leica Microsystems), imaged with a CCD camera using IM500 (Leica) and cropped in Adobe Photoshop.

Determination of BAC Transgene Copy Number by qPCR. The number of copies of each transgene in the genome of founder animals was measured by qPCR using DyNAmo SYBR Green (Finnzymes) and standard procedures. Genomic DNA was isolated as described (4), precipitated with ethanol and resuspended in 10 mM Tris-HCl, pH 8.5. Genomic DNA from different mouse samples was measured by UV spectrophotometer and adjusted to 5 ng/μL. PCR reactions were performed in duplicate in 20 μL using 96-well plates (Bio-Rad) in a qPCR thermocycler (Chromo4 with OpticonMonitor software, Bio-Rad), containing primers that recognize both WT and TG sequences. Specific primers that detect only endogenous WT receptor gene (as for genotyping LuRKO mice) were also used for normalization of the samples and standardization of TG copy numbers. A linear standard curve was drawn using WT genomic DNA at different dilutions. Considering that WT genome contains 2 copies of the *LHR* gene, the extra number of copies in the founder TG animals was considered as TG copies according to the trend line equation and dilution used. The following conditions were used: 95 °C for 15 min, followed by 40 cycles of 94 °C for 20 s, 56 °C for 45 s, 72 °C for 1 min, 80 °C for 1 s.

Cell Cultures and Transfections. To analyze the ability of the LHR^{LH-} and LHR^{cAMP-} mutants to generate cAMP signal, either basally or in response to hCG, HEK-293 cells previously seeded onto 96 well plates were transfected with high dose of 100 ng of the receptor cDNAs, using Lipofectamine 2000 (Invitrogen) transfection reagent. cAMP generation was monitored by cotransfection with 40 ng of a cre-luciferase plasmid DNA, and using 5 n of pRL-CMV as a transfection control. The total concentration of transfected DNA was standardized using pcDNA 3.1. Forty-eight hours after transfection, cells were stimulated with 0, 0.05, 0.5 and 5 nM hCG for 4 h and assayed for cre-luciferase and pRL-CMV activity using Luclite substrate solution (Perkin-Elmer), and coelenterazine substrate (Calbiochem) respectively. Luminescence was determined using a Victor2 plate-reading Luminometer (Perkin-Elmer). In another experiment, plasmids encoding β2-adrenergic receptor (β2-AR) and the LHR^{cAMP-} mutant were cotransfected (100 ng of each) with cre-luciferase plasmid as above, and assayed for luciferase activity in the absence and presence of 0.05 and 0.5 nM hCG.

Immunofluorescence Staining of Tagged Receptors by Confocal Imaging. Visualization of the tagged LHR molecules was carried out using indirect immunofluorescence microscopy of HEK-293 cells stably transfected with *N*-terminally tagged LHR either HA-WT, HA-LHR^{LH-} or FLAG-LHR^{cAMP-}. Surface receptors were labeled by 'feeding' the live intact cells either with a rabbit anti-FLAG antibody (1:500, Sigma) or mouse anti-HA antibody (1:250, Covance) for 20 min at 37 °C, before fixation (4% paraformaldehyde in PBS, 20 min), followed by incubation for an additional 15 min in the absence (nonpermeabilized) or presence of the 0.02% Nonidet P-40 in PBS with 2% FBS for 15 min (permeabilized). Cells were then washed extensively with PBS and further incubated for 30 min with goat anti-mouse or goat anti-rabbit Alexa Fluor 488-conjugated antibodies (1:1000, Invitrogen) in blocking solution. Specimens were washed extensively in PBS, mounted on

glass slides, and examined using a Leica SP5 laser scanning confocal microscope with a 63×/1.4NA oil immersion objective, using instrument settings verified to produce negligible bleed through between channels and an estimated section thickness of 1 μm. Micrographs shown are representative optical sections imaged through the center of the cell.

Immunoprecipitation. HEK-293 cells expressing either or both *LHR* mutants, or both LHR^{-cAMP} and β2-AR (a gift from Mark von Zastrow, Univeristy of California San Francisco) were washed 48 h after transfection, and collected using lysis buffer with protease inhibitors (50 mM Tris-HCl, pH 7.4, with 150 mM NaCl, 1 mM EDTA, and 1% TRITON X-100). The extracts were incubated on ice for 20 min followed by microfuge centrifugation for15 min at maximal speed. Protein concentrations in the supernatants were measured using the Bradford assay. For coimmunoprecipitation of differentially tagged LHRs, and differentially tagged LHR^{-cAMP} and β2-AR, one-mL aliquots of cell lysates were incubated overnight with 40 μL of anti-FLAG agarose affinity gel (A2220; Sigma) and then eluted with FLAG peptide (F4799; Sigma). Immunoprecipitates were separated by SDS polyacrylamide-gel electrophoresis (SDS/PAGE) under reducing conditions, electroblotted onto a nitrocellulose membrane, probed with either an anti-FLAG antibody (F7425; Sigma) or an anti-HA antibody (sc-805; Santa Cruz Biotechnology), and horseradish peroxidase-conjugated goat anti-rabbit IgG (DAKO). The immunoreactive bands were visualized using an ECL detection system (Amersham Biosciences).

mRNA Expression by qPCR. Quantitative PCR was performed by standard protocols using DyNAmo SYBR Green (Finnzymes) kit. PCR reactions were performed in triplicate in 20 μL using 96-well plates (Bio-Rad) in a qPCR thermocycler (Chromo4 with OpticonMonitor software, Bio-Rad), using primers that recognize LHR (WT and mutants, see below). For normalization of the samples a housekeeping gene (*Ppia*) was used. A linear standard curve was drawn using different dilutions of a plasmid containing the cDNA of the LHR. Results are expressed as the number of *LHR*/*Ppia* versus WT control.

The same procedure was used to determine the level of expression of LH-dependent Leydig cell-specific *StAR* and *Cyp17a1* genes in testes of the different mutant mice, and result are presented below as percentage of WT controls.

LHR Binding Measurements. [^{125}I]-hCG binding to testicular homogenates was measured as previously described (5, 6). Briefly, a piece of the frozen testis (see above) was homogenized with an Ultra-Turrax 18/10 homogenizer in Dulbecco's PBS (100 mg testis/mL) containing 0.1% (wt/vol) BSA (Sigma Chemical), and 100 μL aliquots were used for binding measurements. A 1–3 nM concentration of [^{125}I]-hCG (20-50 μCi/μg, Perkin-Elmer) was used in single-point measurements, to assess the binding capacity of the testis tissue. Specific binding was calculated from the difference of binding in the absence and presence of a 1000-fold excess unlabeled hCG (Pregnyl, Organon). For construction of binding-inhibition curves, 100 μL aliquots of LHR cDNA-transfected HEK-293 cells (about 0.2×10^6 cells) were incubated (in triplicates) in the presence of 0.3 nM [^{125}I]-hCG and increasing concentrations of cold hCG (0-10 nM). Incubations were terminated by addition of 4 mL ice-cold Dulbecco's PBS-BSA. Bound and free hormone were separated by centrifugation at 3,000 *x g* for 30 min. The supernatants were discarded, and the radioactivity in the pellets was measured in a γ-counter (1470 Wizard, Wallac).

Measurement of Tubule Diameter and Leydig Cell Volume Density. Tubule diameters and Leydig cell volume densities of testis samples were measured from paraffin sections stained with eosin-hematoxylin using a Leica microscope and Leica IM1000 software (Leica). Sections from three animals per group were analyzed, all tubules in three sections were measured. In the same way, Leydig cell volume densities were measured and calculated as percentage (%) of the total area of the section.

Oligonucleotides. All of the short primers (20–30 nts) described in this paper were purchased from TAG. All longer primers (60–140 nts) were purchased from Thermo.

LHR cDNA mutants. The primers used to create the C22A, (LHR^{LH-}) mutant:

5′-GCCGGATGGTGCCCTGCGCGCACCTGGCCCTCGAGCTGGC-3′ and 5′-GCCAGCTCGAGGGCCAGGTGCGCGCAGGGCACCATCCGGC-3′.

The primers used to create DTM67 (LHR^{cAMP-}) mutant:

5′-ACGTTAGGATATACTTTGCAACAACCTACACCTCCAAGAG-3′ and 5′-CTCTTGGAGGTGTAGGTTGTTGCAAAGTATATCCTAACGT-3′.

Primers used to insert FLAG epitope:

5′-CACAGCTGCACTCTGATTACAAAGATGATGATGATAAGCCAGAGTTGTCAGGGTCG and 5′-CGACCCTGACAACTCTGGCTTATCATCATCTTTGTAATCAGAGTGCAGCTGTG.

Primers used to insert HA epitope:

5′-CACAGCTGCACTCTTACCCATACGATGTTCCAGATTACGCTCCAGAGTTGTCAGGGTCG and 5′-CGACCCTGACAACTCTGGAGCGTAATCTGGAACATCGTATGGGTAAGAGTGCAGCTGTG.

For modification of the LHR gene in BAC clones using Red/ET recombination. Selection/counter selection cassette, *RpsL*-Neo, (CS) was amplified with primers containing homology arms for the region to be modified, then *RpsL*-Neo cassette was exchanged by a single strand (ss) oligonucleotide.

For point mutation, LHRLH−. CS-LHR^{LH-}-F 5′-AGGGTCGCGCTGCCCTGAGCCCTGCGACTGCGCGCCGGATGGTGCCCTGCGCGGCCTGGTGATGATGGCGGGATCG-3′; CS-LHR^{LH-}-R 5′-GACCTGGGGCGCCCTGTACTCACAGTCGGGCGAGGCCAGCTCGAGGGCCAGGTCAGAAGAACTCGTCAAGAAGGCG-3′; ssLHR^{LH-} 5′-GGTCGCGCTGCCCTGAGCCCTGCGACTGCGCGCCGGATGGTGCCCTGCGCGCCCCTGGCCCTCGAGCTGGCCTCGCCCGACTGTGAGTACAGGGCGCCCCAGG-3′

For ΔTM67, LHR^{cAMP-}. CS-LHR^{cAMP-}-F 5′-GCAGTGGCCTTTGTCGTCATCTGTGCTTGCTACGTTAGGATATACTTTGCAGGCCTGGTGATGATGGCGGGATCG-3′; CS-LHR^{cAMP-}-R 5′-GGGGGGGGGGAGGGAGAGGTTACTGAATTAACACTCTTGGAGGTGTAGGTTGTCAGAAGAACTCGTCAAGAAGGCG-3′; ssLHR^{cAMP-} 5′-GTGGCCTTTGTCGTCATCTGTGCTTGCTACGTTAGGATATACTTTGCACAACCTACACCTCCAAGAGTGTTAATTCAGTAA-3′

For insertion of the reporter genes. Both reporter genes (eCFP and RFP) were amplified by PCR from bicistronic vectors containing a common IRES and polyA, which were used for the primer binding sites. Reporter gene insertion after the *LHR* gene were performed before other modifications using the following primers:

IRES-XFP-LHR-F 5′-CCATAGTGCACTGTCAACAACCTACACCTCCAAGAGTGTTAATTCAGTAACCTCTCCCTCCCCCCCCCTAAC-3′; and IRES-XFP-LHR-R 5′-TTTGGGTGGACTTTTTTGGGGGGAACATATTTAGATACAATTCAGTAATGGCAGTGAAAAAAATGCTTTATTTG-3′.

Insertion of the *PRL* signal sequence by ALFIRE

ALFIRE-LHR-F 5′-GTCCAGCATACTGGCCTAGCCACCGGAGCTCACACTCAGGCTGGCGGGCCATGGACAGCAAAGGTTCGTCGCAGAAAGGGTCCCGCCTGCTCCTGCTGCTAGGGATAACAGGGTAATGGCCTG-3′; and ALFIRE-LHR-F 5′-GGACCTGGGGCGCCCTGTACTCACAGTCGGGCGAGGCCAGCTCGAGGGCCAGGGCAGCGCAGGGCGCCGTCGGGCACGCAGTTGCAGGGCTCAGGGCAGGATTGGCACAAGAATTACCCT-3′

Primers for genotyping

IRESF 5′-GTATTCAACAAGGGGCTGAAGG-3′; CFP-R 5′-TTGATCCTAGCAGAAGCACAGG-3′; and RFP-R 5′-CCATGGTCTTCTTCTGCATCAC-3′

Primers for RT-PCR

F1 5′-TACCCTTACAGTCATCACTCTGGA-3′; and R1 5′-TTCAAGAAGCTTCCAGAGGAAC-3′

Primers for qPCR (TG copy number)

F1 5′-AGCATCTGTAACACAGGCATCC-3′; and R1 5′-CACAGCGTGATGGACTCATTAT-3′

Primers of qRT-PCR

Total mLHR expression

F 5′-AGCATCTGTAACACAGGCATCC-3′; and R 5′-CACAGCGTGATGGACTCATTAT-3′

Primers for *StAR* (GenBank NM_011485)

F 5′-CAGGGAGAGGTGGCTATGCA-3′; and R 5′-CCGTGTCTTTTCCAATCCTCTG-3′

Primers for *Cyp17a1* (GenBank NM_007809)

F 5′-GGCCCCAGATGGTGACTCT -3′; and R 5′-GGACTCCCCGTCGTATGTAA -3′

Primers for housekeeping gene peptidylprolyl isomerase A (*Ppia,* GenBank NM_008907)

F 5′-CATCCTAAAGCATACAGGTCCTG-3′; and R 5′-TCCATGGCTTCCACAATGTT-3′

SI Results

Weights of the LuRKO, LHR^{LH-} and LHR^{cAMP-} testes were approximately one third of those of WT mice, whereas the $LH^{LH-/cAMP-}$ testes did not differ from the latter (Table S3). Seminal vesicles of the LuRKO, LHR^{LH-} and LHR^{cAMP-} mice were rudimentary, whereas the WT and $LHR^{LH-/cAMP-}$ seminal vesicles had similar weights (Table S3).

Seminiferous tubular diameters and Leydig cell volume densities of the LuRKO, LHR^{LH-}, and LHR^{cAMP-} testes were similar and narrower/smaller than in the $LHR^{LH-/cAMP-}$ and WT testes, which did not differ from each other (Table S4).

Transgene copy numbers were similar in the LHR^{LH-} (3–11) and LHR^{cAMP-} (2–8) mice (Table S1).

With maximal amounts (100 ng) of LHR^{LH-} or LHR^{cAMP-} plasmids were transfected into HEK-293 cells, no cAMP signal (measured by cre-luciferase activity) was detected either in the absence or presence of hCG (0.05, 0.5, and 5 nM) (Fig. S2), indicating that overexpression of one of the mutants alone is not able to activate cAMP generation, which was readily detected in cells expressing WT receptor. Likewise, cotransfection (100 ng each) of the LHR^{cAMP-} mutant and β2-AR expression plasmids did not produce cAMP signal basally or in response to hCG stimulation (Fig. S2). Robust activation of signaling was observed in each case when WT LHR was transfected.

Total mLHR expression of different mutants was compared to WT controls, whereas LHR single mutants express ∼60% of control levels, the double mutant ($LHR^{LH-/cAMP-}$) overall expresses 2.3 times the LHR levels than WT (Table S2).

LH-dependent Leydig cell-specific genes (*StAR* and *Cyp17a1*) were analyzed by quantitative PCR to show the direct activation of cell signaling in Leydig cells by LH. Negligible expression of either gene could be detected in LHR single mutants and LuRKO mice samples, whereas $LHR^{LH-/cAMP-}$ and WT expressed both genes (Table S5) at near similar levels.

1. Zhang Y, Muyrers JP, Rientjes J, Stewart AF (2003) Phage annealing proteins promote oligonucleotide-directed mutagenesis in Escherichia coli and mouse ES cells. *BMC Mol Biol* 4:1.
2. Rivero-Müller A, Lajić S, Huhtaniemi I (2007) Assisted large fragment insertion by Red/ET-recombination (ALFIRE)—an alternative and enhanced method for large fragment recombineering. *Nucleic Acids Res* 35:e78.
3. Ji I, et al. (2004) Trans-activation of mutant follicle-stimulating hormone receptors selectively generates only one of two hormone signals. *Mol Endocrinol* 18:968–978.
4. Ballester M, Castelló A, Ibáñez E, Sánchez A, Folch JM (2004) Real-time quantitative PCR-based system for determining transgene copy number in transgenic animals. *Biotechniques* 37:610–613.
5. Catt KJ, Ketelslegers J-M, Dufau ML, National Institute of Child Health and Human Development (1976) *Receptors for Gonadotropic Hormones* (Dekker, New York), pp 175–250.
6. Huhtaniemi IT, Nevo N, Amsterdam A, Naor Z (1986) Effect of postnatal treatment with a gonadotropin-releasing hormone antagonist on sexual maturation of male rats. *Biol Reprod* 35:501–507.
7. Sangkuhl K, Schulz A, Schultz G, Schöneberg T (2002) Structural requirements for mutational lutropin/choriogonadotropin receptor activation. *J Biol Chem* 277: 47748–47755.

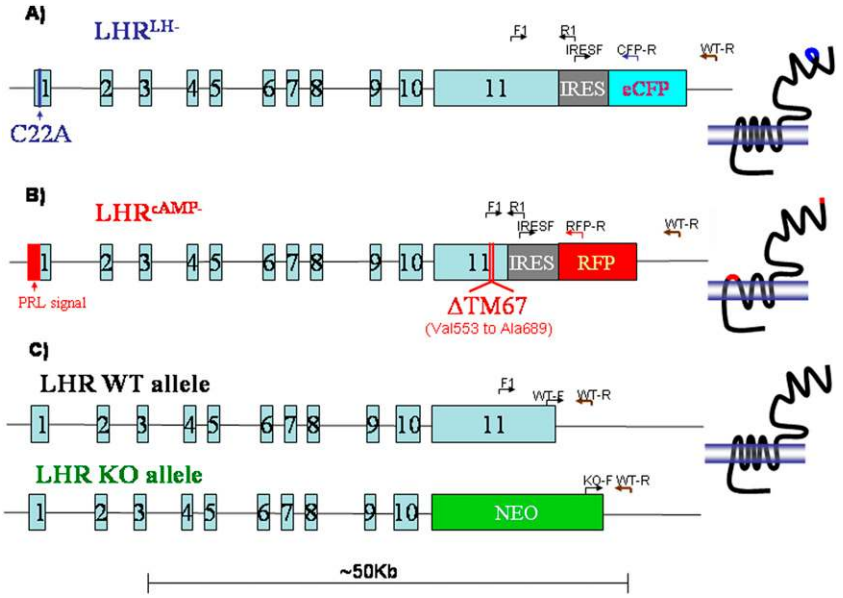

Fig. S1. Details of the BAC constructs used to express binding- and signaling-deficient LHR mutants in transgenic mice. BAC clones containing the entire *LHR* genomic gene (exons numbered) were modified by point mutations, insertions, and deletions of specific areas. (*A*) One receptor mutant harbored an inactivating mutation in the LH/hCG ligand binding region (LHR^{LH-}), where Cys^{22} was replaced by Ala^{22} (C22A) through a TGC/GCA point mutation. As reporter gene, a bicistronic cassette containing an internal ribosomal entry site (IRES) and enhanced cyan fluorescent protein (eCFP) were inserted after the *LHR* gene. (*B*) The other mutant contained a deletion of transmembrane domains 6 and 7 (ΔTM67) in exon 11 (amino acid deletion Val^{553} to Ala^{689}), which are involved in G protein coupling and second messenger production (7) (LHR^{cAMP-}) but retaining the intracellular domain. To ensure translocation of the latter LHR mutant to the cell membrane, a bovine prolactin (PRL) leader signal was inserted into the N-terminus of the mature receptor. As reporter gene, a bicistronic cassette containing an IRES and *Dicosoma* sp. red fluorescent protein (RFP), was inserted after the *LHR* gene. Primer positions are marked, for genotyping: IRESF for either transgene, with RFP-R for LHR^{LH-}-IRES-eCFP, and with CFP-R for LHR^{cAMP-}-IRES-RFP. (*C*) WT and LHR-knockout (LuRKO) alleles, and resulting WT receptor, no protein is generated by the LuRKO allele. Primers for genotyping the *LHR* knockout (LuRKO) and WT alleles were as previously described and shown in the figure to demark a different position. Primers F1-R1 were used for RT-PCR amplification of either transgene because LHR^{cAMP-} encoded a shorter product. Schematic representation of each of the receptor mutants is portrayed on the right of the BAC diagrams marking, with blue and red colors the areas of modification.

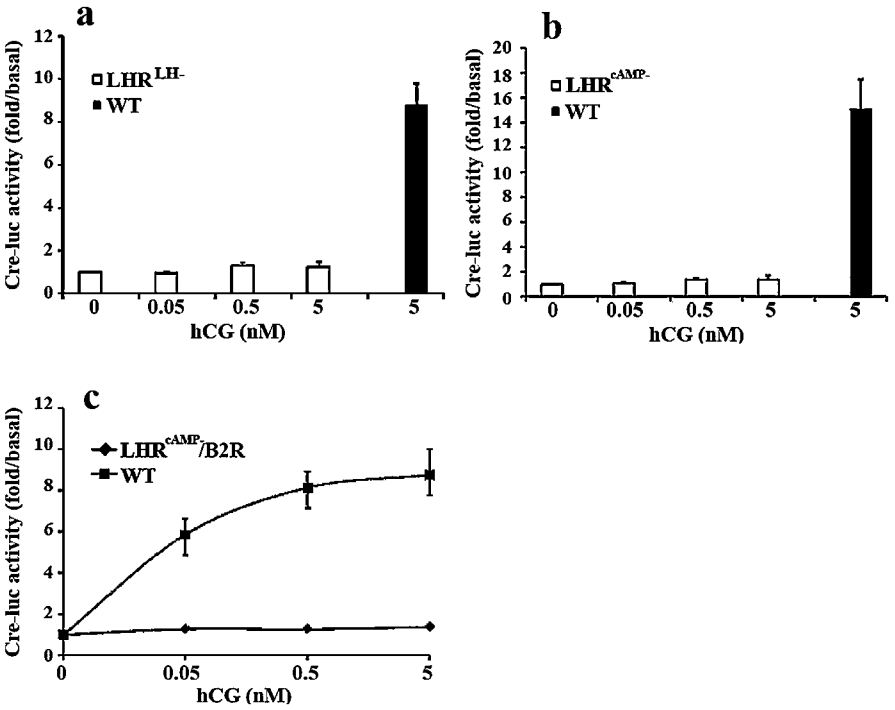

Fig. S2. Inactive LHR mutants are unable to respond to hCG or to *trans*-activate other GPCRs. LHR^{LH-} (*A*) or LHR^{cAMP-} (*B*) plasmids (100 ng per well) were transfected into HEK-293 cells together with the cAMP-cre-luciferase activity plasmid, and then cells were stimulated with different concentrations of hCG (0.05, 0.5, and 5 nM) but showed no cAMP response. (*C*) Cotransfection of LHR^{cAMP-} with β2 adrenergic receptor (β2R) expression plasmids in HEK-293 cells did not produce cAMP signal basally or in response to hCG stimulation (0, 0.05, 0.5, and 5 nM). A clear cAMP response was observed in each experiment in cells transfected with WT LHR.

Table S1. Transgene copy number

TG founder	TG copy number
LHR^{LH-}	3–11
LHR^{cAMP-}	2–8

Genomic DNA of two founder mice per group in duplicate was analyzed by real-time PCR. Copy numbers were calculated after subtraction of the WT copy number (considered = 2) and calculated on a linear standard curve created by dilutions of WT genomic DNA.

Table S2. LHR expression

	Total LHR expression, times WT
LuRKO	N/A
LHR^{LH-}	0.58 ± 0.24^{a}
LHR^{cAMP-}	0.68 ± 0.29^{b}
$LHR^{LH-/cAMP-}$	2.33 ± 0.64^{c}
WT	1.00 ± 0.19^{b}

Testicular mRNA was isolated and analyzed by real-time PCR for LHR expression, normalized with a housekeeping gene (*Ppia*), and presented as total LHR expression as compared to control (WT). Results are the mean ± SD of at least three different samples per group, each sample measured in triplicate. Values with different superscript letters differ statistically significantly ($P < 0.05$).

Table S3. Testis and seminal vesicles weights

	Testis, mg	Seminal vesicles, mg
LuRKO	53.6 ± 5.7^{a}	N/A
LHR^{LH-}	52.1 ± 8.3^{a}	N/A
LHR^{cAMP-}	54.9 ± 6.7^{a}	N/A
$LHR^{LH-/ cAMP-}$	145.3 ± 44.0^{b}	539.8 ± 37.7^{a}
WT	147.9 ± 40.2^{b}	535.2 ± 26.6^{a}

Each value is the mean ± SD of measurements from at least four mice. Groups with different superscripts differ significantly ($P < 0.001$). N/A, not applicable because the size of the seminal vesicles in LuRKO, LHR^{LH-}, and LHR^{cAMP-} mice was too small for accurate measurement.

Table S4. Seminiferous tubule diameter and Leydig cell volume densities

Genotype	Seminiferous tubule diameter, nm	Leydig cell volume density, as % of the total area of a testicular section
LuRKO	98.9 ± 11.0^{a}	1.58 ± 0.18^{a}
LHR^{LH-}	100.4 ± 13.9^{a}	2.69 ± 0.16^{a}
LHR^{cAMP-}	95.4 ± 12.2^{a}	2.70 ± 0.20^{a}
$LHR^{LH-/ cAMP-}$	138.2 ± 11.0^{b}	5.49 ± 0.52^{b}
WT	127.8 ± 8.1^{b}	5.47 ± 0.36^{b}

Each value is the mean ± SD of at least three samples. Groups with different superscripts differ significantly ($P < 0.001$ for seminiferous tubular data; $P < 0.05$ for Leydig cell data). Leydig cell volume density (% of total section) was calculated as the area covered by Leydig cells in a testicular histological section divided by the total area of the section.

Table S5. LH-dependent gene expression

	StAR/Ppia	*Cyp17a1/Ppia*
LuRKO	0.059 ± 0.017^{a}	0.077 ± 0.034^{a}
LHR^{LH-}	0.062 ± 0.015^{a}	0.096 ± 0.027^{a}
LHR^{cAMP-}	0.076 ± 0.036^{a}	0.053 ± 0.006^{a}
$LHR^{LH-/ cAMP-}$	0.85 ± 0.15^{b}	0.60 ± 0.13^{b}
WT	1.0 ± 0.084^{b}	1.0 ± 0.17^{b}

Isolated mRNA from testis of different animals was analyzed by real-time PCR, normalized with a housekeeping gene (*Ppia*), and presented as percentage of WT control. Results are the mean ± SD of at least three different animals per group, each analyzed in triplicate. Values with different superscript letters differ statistically significantly ($P < 0.05$).